Received November 3, 2021, accepted November 15, 2021, date of publication November 17, 2021, date of current version November 30, 2021.

Digital Object Identifier 10.1109/ACCESS.2021.3128999

Robust Coordination Scheme for Microgrids Protection Based on the Rate of Change of Voltage

MOHAMED AHMED DAWOUD[1], DOAA KHALIL IBRAHIM[1], (Senior Member, IEEE), MAHMOUD IBRAHIM GILANY[1], AND ABOUL'FOTOUH EL'GHARABLY[2]

[1]Electrical Power Engineering Department, Faculty of Engineering, Cairo University, Giza, Cairo 12613, Egypt

[2]Electrical Power and Machines Department, Higher Institute of Engineering, El-Shorouk City, Cairo 11837, Egypt

Corresponding author: Doaa Khalil Ibrahim (doaakhalil73@eng.cu.edu.eg)

ABSTRACT The wide application of microgrid concept leads to challenges for the traditional protection of distribution networks because of the changes in short circuit level and network topology during the two modes of microgrid operation. This paper proposes a promising solution for these problems by offering a new protection coordination scheme not affected by the variation of short circuit level or the changes in network topology. The proposed protection scheme is based on local measurements at relay location with low sampling frequency by computing the rate of change of fundamental voltage (*ROCOV*) to detect different fault types, identify the faulty zone accurately and guarantee robust coordination between primary and backup relays. The proposed coordination scheme can be achieved by optimizing either two settings for relay characteristic (time dial setting and pickup value) or four settings (time dial setting, pickup and the parameters that control the characteristic shape (A & *B*)). The proposed scheme is extensively tested using MATLAB simulations on the modified IEEE 14 bus meshed network embedded with synchronous/inverter-based distributed generation units under wide variations in operating conditions and short circuit levels for both grid-connected and islanded modes of operation. The achieved results confirm that the proposed coordination scheme can maintain the coordination between primary and backup relays for different fault locations, types and different topologies. It provides selective, reliable, and secured microgrid operation compared with conventional schemes, using fault current limiters and some other techniques discussed in the literature.

INDEX TERMS Coordination scheme, distributed generation, local measurements, microgrid and rate of change of voltage (*ROCOV*).

I. INTRODUCTION

A microgrid has become increasingly popular as an attractive solution for more sustainable and greener production of energy. It offers on-site power generation at the consumption point with improved reliability and reduced distribution losses [1].

Despite the numerous benefits of the microgrid with distributed generation (DG) integration, the protection challenges become serious concerns, where the performance of the traditional protection coordination schemes may be ineffective when applied to microgrids since they are susceptible to malfunctions and false tripping [2]. The protection relay faces substantial difficulties as the fault current magnitude varies significantly depending upon the size, type and location of DG [3]. Furthermore, dynamically changing load, generation and network topology cause a significant change in fault currents which sometimes results in a miscoordination of one or more primary and backup traditional directional overcurrent relays (DOCRs) that are commonly used as main protection relays of microgrid networks. Such miscoordination results in unwanted false tripping for some healthy feeders and loads [4].

The available techniques in the literature for keeping the relays coordinated in both grid and islanded modes can be classified into local and communication based approaches. The schemes of the first category do not need communications [5]–[10]. In [5], due to the difference in fault

The associate editor coordinating the review of this manuscript and approving it for publication was Bin Zhou.

magnitudes for grid-connected and islanded operation, fault current limiters (FCLs) are positioned and traditional DOCRs are optimally coordinated considering both microgrid modes of operation. By using FCLs, the infeasibility of conventional DOCRs to provide proper protection coordination was overcome; however, the coordination is violated with any change in the network operating conditions. A thyristor-based scheme is proposed in [6] to identify a distribution system operating condition and adapt the overcurrent protection of the grid. In that scheme, the system equivalent impedance is estimated, which differs for islanded or connected-operating conditions. Then, the pre-determined suitable setting is selected without any communications. However, that scheme is not effective with any variation in the system operating circumstances. A time-current-voltage characteristic (TCVC) is also proposed in both grid-connected and islanded modes of operation in [7]. The TCVC uses the faulted phase voltage and current magnitudes for determining the operating time of the relay. The TCVC does not require any communication system and achieves a notable reduction in total relay operating times. However, optimal settings of overcurrent relays are needed for every change in network topology. Moreover, the scheme is only tested with synchronous-based DG units and solid faults are only assumed. It may not be effective in a system that is dominated by inverter-based DG units due to their low fault current contribution. A voltage-based protection method for distribution systems with DG is proposed in [8]. In which, the relay characteristic is formulated from extensive analysis for voltage behavior during fault conditions. The method is communication-less and independent of mode of operation. However, it is very sensitive to any slight changes in voltage, thus leading to potential maloperation. Non-unit protection method is also investigated in [9] for fault discrimination within DC microgrid systems. It analytically studies the current and voltage signals, their rate of change (*ROCOI*, *ROCOV*) and impedance profiles as measured at the generator converter terminals. In that study, there is no effective coordination method between primary and backup relays. The method is investigated for two fault locations only. When the fault conditions change, the protection relays cannot achieve the selectivity criteria since the fault location is based on constant threshold values. Another recent scheme for microgrid protection is introduced in [10] depending on dual protection settings for DOCRs. The first setting of TDS for primary protection is based on the very inverse curve while the second setting for backup protection is based on the normal inverse curve. The results show its superior performance over the conventional dual setting method by reducing the total operating time. Besides, the protection method does not require any communication links between relays. However, the method is still dependent on DOCRs and has not been evaluated under the wide variation in the short circuit levels under the changes in the operating conditions of the microgrid. Therefore, the pickup current and TDS need to be re-adjusted again under any changes in the operating conditions. Also, the method is not been tested with different types of DG.

On the other hand, several microgrid protection schemes that rely on communications have been proposed in [11]–[21]. Adaptive settings of the relays have been applied in [11]–[13], where these schemes require a direct or indirect communication channel to reset the relays settings according to the prevailing conditions such as operational or topological changes. In [13], an adaptive protection coordination scheme has been discussed based on a centralized controller running the real time analysis of the data received from the intelligent electronic devices. The wide area monitoring system is implemented by the application of phasor measurements units and implemented for all nodes and branches of the AC grid in [14]. A differential protection strategy is developed using data mining techniques which relies on communicating measurements between two relays of the protected feeder [15], [16]. In [17], a travelling wave based protection scheme that utilizes a low bandwidth communication for meshed distribution systems with DG operating as a microgrid was proposed. In [18], [19], dual setting DOCRs have been applied for meshed distribution systems with DG. Relays are coordinated in such a way to reduce the overall relay operating time for grid-connected and islanded modes. As clearly shown, the communication system plays an important role in the adaptive protection methods. The cost, speed, redundancy, and reliability of the communication systems are vital factors that must be considered before implementing an adaptive protection method [20], [21]. Besides, the communication failure may lead to the inability of protection scheme [8].

Some other research studies were conducted towards applying the rate of change of the phasor voltage (*ROCOV*) in islanding detection and distance protection. In [22]–[24], the rate of change of voltage and other parameters are used to detect the islanding condition at the point of common coupling between the distributed generation units and distribution networks. These algorithms are applied to detect DG operating modes correctly and quickly. Also, the conventional distance relay performance is enhanced when the *ROCOV* feature is added in [25]–[27]. Such algorithm can distinguish accurately the faulty cases and the stressed conditions. In fact, the above methods are not designed to handle the coordination of primary and backup relays to ensure secured feeder protection in microgrids.

Figure 1 summarizes most of the microgrid protection approaches in literature with the general features and limitations of each category. Through the different research studies arranged schematically in Fig. 1, it can be deduced that there is an urgent need to propose a coordination approach which does not depend on the current as the current changes significantly with the changes occurring in microgrid topology. It is also necessary for the required proposed approach to avoid using communication systems to change relay setting

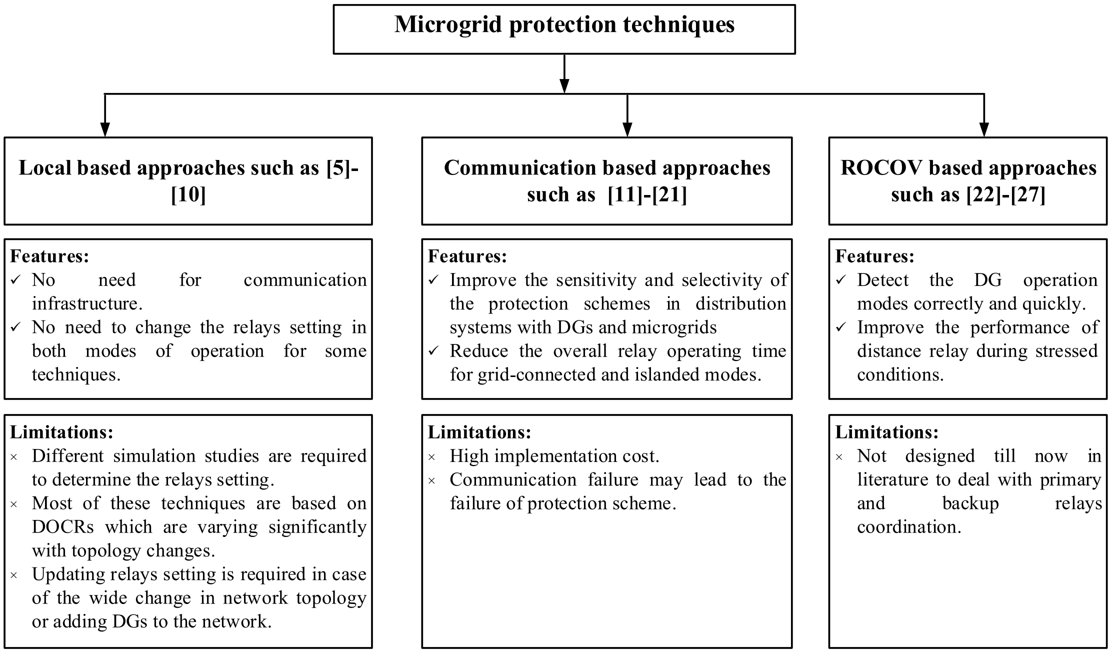

FIGURE 1. Research directions for microgrid protection techniques.

frequently since it reduces system reliability and it has a high cost as well.

The main contribution of this paper is to propose a robust protective coordination scheme suitable for microgrids. The proposed coordination scheme is formulated here as an optimization problem for each mode of operation: grid-connected and islanded modes. The protection scheme is based on computing the rate of change of fundamental voltage (*ROCOV*) to discriminate and locate the faulty section relying on local measurements only. The main feature of the new proposed coordination scheme is that it will not be affected by any variation of the network topology or short circuit level. It must be pointed out that *ROCOV* relay was developed by the authors in [28] and fully examined with simulation and practical implementations. As deduced in [28], *ROCOV* relay is stable during transient healthy conditions and provides a selective, reliable, and sensitive protection system in case of faults in distribution systems compared to conventional relays (overcurrent and under voltage relays).

The organization of this paper is presented as follows: description of the proposed protection scheme is offered in Section II. It briefly offers the basic idea of *ROCOV* relay, and then the problem formulation for *ROCOV* relays coordination is described. Test system description and the optimum settings of proposed protection scheme are presented in Section III. Simulation results for evaluating the proposed protection scheme on modified IEEE 14 bus system with wide variation in short circuit levels are discussed in Section IV. Comparison between the proposed scheme and other techniques is presented in Section V. Proposing user-defined characteristics for microgrid protection coordination using *ROCOV* relays is described in Section VI. Finally, the conclusions are drawn in Section VII.

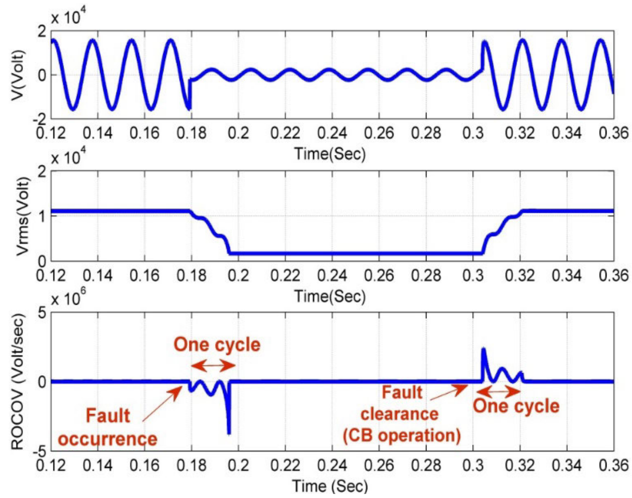

FIGURE 2. Sinusoidal voltage, RMS voltage and *ROCOV* in case of a fault occurs at 0.18 s and cleared at 0.3 s.

II. DESCRIPTION OF THE PROPOSED PROTECTION SCHEME

In this section, the *ROCOV* relay for fault detection and the proposed coordination scheme formulation for grid-connected and islanded modes are presented.

A. DESCRIPTION OF THE ROCOV RELAY

The proposed scheme is based on the fact that the rate of change of the fundamental voltage is close to zero under normal operating conditions while it jumps to higher values under fault conditions at the fault instant. Fig. 2 shows the voltage (sinusoidal and RMS) and *ROCOV* waveforms at relay R1 during a fault at the mid-point of feeder 1 (F1) in

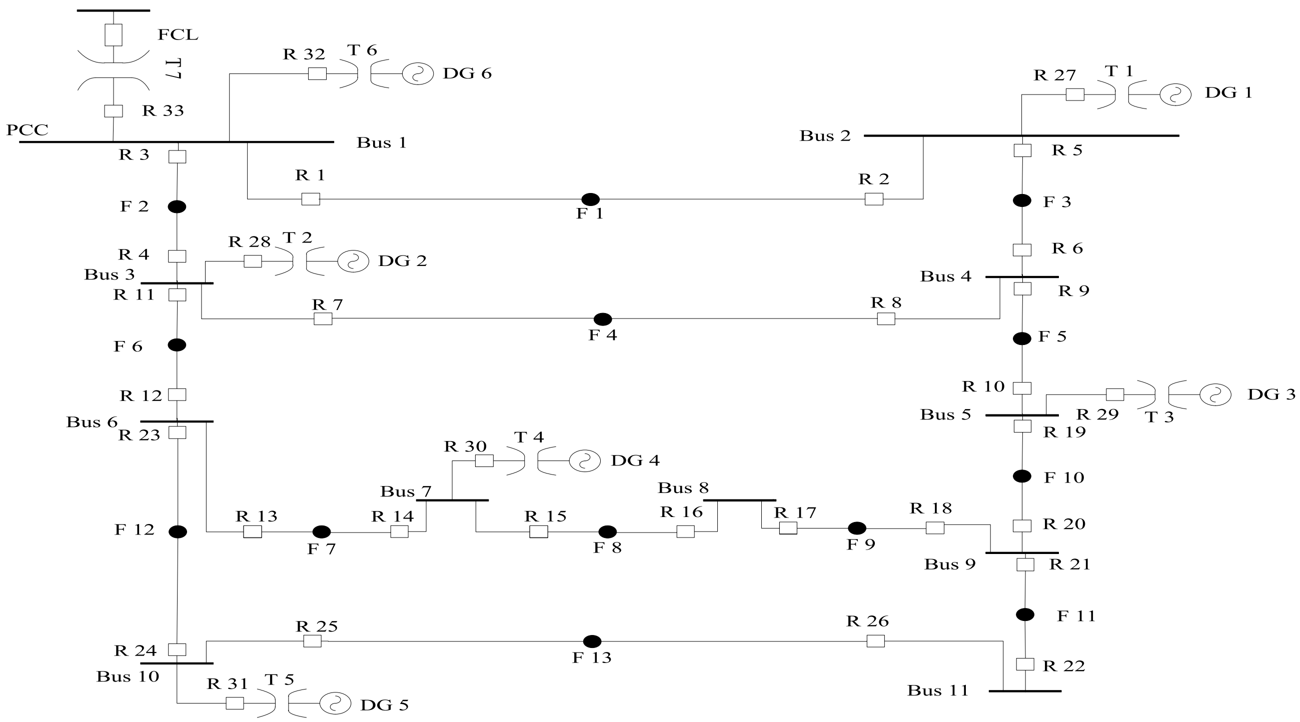

FIGURE 3. **Modified IEEE 14 bus system embedded with DG units.**

the modified IEEE 14 bus system [5]. The feeder number and the fault location have the same number in the figure. This system is illustrated later in Fig. 3. The fault has occurred at 0.18 s and cleared at 0.3 s. As shown, the value of *ROCOV* is negative at the instant of fault occurrence (voltage reduction), while it has a positive value at the instant of fault clearance (voltage increase). The relay needs only one post-fault cycle (which represents the required detection time) of voltage waveform to verify the fault occurrence. The changes in RMS and *ROCOV* during the first cycle after fault occurrence are illustrated in Fig. 2.

Such *ROCOV* value can be calculated using the following equation:

$$ROCOV = \frac{V_{A1(n)} - V_{A1(n-1)}}{\Delta T} \tag{1}$$

where: $V_{A1(n)}$ and $V_{A1(n-1)}$ are the calculated RMS values of fundamental voltage for phase A at present sample (n) and previous one ($n-1$), respectively, while ΔT is the sampling interval.

The *ROCOV* value at relay location is calculated using the pre and post RMS fault voltages during the sampling interval. The proposed *ROCOV* value is a function of fault distance. The *ROCOV* value is also a function of the sampling rate. The higher the sampling rate, the higher the accuracy. In fact, low sampling frequency in the range of 1-20 kHz can be applied to implement the proposed scheme. All results of studied cases in this paper are extracted with 20 kHz sampling frequency.

The *ROCOV* relay is supposed to be installed at the beginning and end of each protected main line section. In the event of a fault in any line section, the line should be disconnected from the beginning and the remote end of the line via installed *ROCOV* relays similar to traditional DOCRs used in the microgrid [5]. However, if the feeding is from one end only, then only one protection device is placed at the beginning of the line section as in radial distribution networks.

As discussed in [28], the relation between the measured *ROCOV* values and the relay operating time takes the same shape of the standard inverse-time characteristics of DOCR. Hence, a similar equation is used to describe this relation as given in (2).

$$t(op) = TDS\left[\frac{A}{\left[\frac{ROCOV_{SC}}{ROCOV_{pick-up}}\right]^{B} - 1}\right] \tag{2}$$

where:

- t(op): is the operating time of the *ROCOV* relay.
- *TDS* : is the time dial setting of the *ROCOV* relay.
- $ROCOV_{SC}$: is the maximum measured rate of change of fundamental voltage during the first cycle after fault occurrence.
- $ROCOV_{pick-up}$: is the setting point value of the *ROCOV* relay determined by normal load switching at relay location.
- A and B: are constants that control the characteristic shape of the *ROCOV* relay.

The setting of *ROCOV* relay in this paper will be designed based on the assumption of single fault occurrence in the relay protection zone, which can be considered a reasonable

TABLE 1. Constants for typical inverse relay characteristics.

Characteristic	A	B
Standard Inverse	0.14	0.02
Very Inverse	13.5	1
Extremely Inverse	80	2

assumption when utilizing only local measurements. The constants A and B can be defined according to typical characteristics of Table 1 [29]. In this paper, A and B are chosen to be 0.14 and 0.02, respectively, to represent similar characteristics to the DOCR standard inverse characteristics. Besides, in Section VI, the coordination problem is also reformulated for optimizing both A and B using user-defined characteristics.

If the calculated *ROCOV* value from (1) exceeds a pickup value, the relay determines the required operation time, t from (2) and trips at the end of the estimated delay. It is worth mentioning that the *ROCOV* relay operates in conjunction with a directional feature (similar to traditional DOCR) in order to act only when the power flow is in the forward direction.

It should be noted that the methodology of the *ROCOV* relay is fully described by the authors in [28]. It is also worth clarifying that the *ROCOV* relay is extensively tested in [28] under different healthy and faulty conditions in distribution systems. The achieved results demonstrate the stability of the *ROCOV* relay under transient healthy conditions including dynamic load (starting transients of induction motors), static nonlinear load and capacitor switching. For all transient healthy conditions, calculated *ROCOV* value was less than the pickup value, and thus the relay does not generate any false tripping signal.

B. PROTECTION COORDINATION SCHEME FORMULATION BASED ON THE ROCOV RELAY

Two groups of settings are required to be stored in the *ROCOV* relay for grid-connected and islanded modes. The switching between the two modes can be easily achieved based on an effective islanding detection technique based on local measurements proposed by the authors in [30].

The protection coordination problem is typically formulated as an optimization problem (similar to typical DOCRs given for example in [18]), where the main objective is to minimize the overall relays operating time for each mode of operation: grid-connected and islanded modes.

For each mode of operation, the objective function T is the sum of the operating times of all *ROCOV* relays for all fault locations which needs to be minimized as follows:

$$Minimize\ T = \sum_{j=1}^{M}\left(\sum_{i=1}^{N}(t_{pij} + \sum_{k=1}^{\substack{all\ backup\\ relays\ for\\ i\ primary\ relay}} t_{bkj})\right) \tag{3}$$

TABLE 2. Settings of *ROCOV* relays for optimum coordination scheme.

Relay No.	Grid-connected mode		Islanded mode	
	TDS s	$\lvert ROCOV_{pick-up}\rvert$ (Volt/s) ×10^5	*TDS* s	$\lvert ROCOV_{pick-up}\rvert$ (Volt/s)×10^5
1	0.7122	2.5250	0.6153	4.0200
2	0.8184	2.7068	0.7343	2.6866
3	0.7169	2.5250	0.7492	2.7068
4	0.8545	2.2220	0.7088	2.1715
5	0.8305	2.7068	0.7486	2.6866
6	0.8987	2.1513	0.7434	2.1210
7	0.8874	2.2220	0.7963	2.1715
8	0.9585	2.1300	0.7906	2.1000
9	0.9624	2.1513	0.8416	2.1210
10	1.0218	2.1715	0.8083	2.1210
11	0.914	2.2220	0.7817	2.1715
12	0.9666	2.1715	0.7947	2.0907
13	1.097	2.1715	0.8779	2.0907
14	1.0124	2.2725	0.8094	2.2220
15	1.1047	2.2725	0.8619	2.2220
16	1.0315	2.2725	0.8483	2.1917
17	1.0792	2.2725	0.8609	2.1917
18	1.0491	2.0705	0.8652	2.0200
19	1.0098	2.1715	0.8422	2.1210
20	1.0646	2.0705	0.8461	2.0200
21	1.0126	2.0705	0.7797	2.0200
22	1.0013	2.7371	0.8156	2.6462
23	0.927	2.1715	0.7488	2.0907
24	1.0637	2.7270	0.8132	2.6260
25	0.9731	2.7270	0.7614	2.6260
26	1.0395	2.7371	0.8056	2.6462
27	0.9211	2.7068	0.8453	2.6600
28	1.0057	2.2220	0.8944	2.1500
29	1.133	2.1500	0.9466	2.1210
30	1.2073	2.2725	0.9648	2.2220
31	1.1642	2.7000	0.9119	2.6000
32	0.8057	2.5000	0.8482	2.6800
33	0.8069	2.5000		

where:

- t_{pij} and t_{bkj} are the operating time of the primary *ROCOV* relay (i) and its all backup *ROCOV* relays (k) respectively for a fault location (j) calculated using (2).
- N represents the total number of relays, while M denotes the total number of fault locations.

The objective function should be achieved while fulfilling the following set of constraints for both modes of operation:

$$t_{bkj} - t_{pij} \geq CTI \quad \forall i, k \tag{4}$$

where CTI is the coordination time interval that must be satisfied to achieve discrimination between the primary (i) and backup *ROCOV* relay (k) for a fault at j. The CTI usually takes a value between 0.2 and 0.5 s; it is set to be 0.2 s in this study. Other constraints include limits on the relays' are presented as follows:

$$ROCOV_{pick-up(min)} \leq ROCOV_{pick-upi} \leq ROCOV_{pick-up(max)} \tag{5}$$

$$TDS_{min} \leq TDS_i \leq TDS_{max} \tag{6}$$

The minimum and maximum pick-up ($ROCOV_{pick-upi}$) depend on the maximum load switching condition at each relay location. As discussed in [31] for DOCRs, the pickup value of *ROCOV* relay can vary between 1.01 and 2 times the maximum value obtained under normal load switching [28]. The TDS_{min} and TDS_{max} are the minimum and maximum limits for relay *i* with values of 0.05 and 1.5 s respectively.

Various optimization methods, including heuristic and exact techniques can be applied to solve the optimization problem to achieve minimum operating time [32]–[33]. The problem is simply solved here using the MATLAB built-in *fmincon* optimization function. The protection coordination problem has been formulated as a non-linear programming (NLP) problem [34], by considering both the time dial and pickup settings to be continuous variables.

III. TEST SYSTEM AND THE OPTIMUM SETTINGS

A. TEST SYSTEM

The modified IEEE 14 bus system with six added synchronous DG units is presented in Fig. 3. The synchronous based DGs are located at buses 1, 2, 3, 5, 7 and 10. The added DGs are rated at 2.4 MVA and 0.9 power factor. Other network parameters and data are presented in [5]. The modified IEEE 14 bus system is chosen in this paper as a test system for the purpose of comparison with the conventional DOCRs protection scheme which applies FCL on the same test system in [5].

B. THE OPTIMUM SETTINGS FOR ROCOV RELAYS

The microgrid operating philosophy is that in normal condition the microgrid is desired to operate in the grid-connected mode but in case of any disturbance, it would seamlessly disconnect from the utility at the point of common coupling (PCC) via relay R33 (shown in Fig. 3) and then continue to operate in the islanded mode [5]. Therefore, the optimum settings for the *ROCOV* relays are calculated for both grid-connected and islanded modes, according to the procedure mentioned in above sections, as presented in Table 2 (33 relays in grid-connected mode and 32 relays in islanded mode).

IV. EVALUATION THE PERFORMANCE OF THE PROPOSED COORDINATION SCHEME

The proposed protection scheme is extensively examined with different fault locations, types and different topologies in the next sections.

A. PERFORMANCE OF PROPOSED COORDINATION SCHEME WITH DIFFERENT FAULT LOCATIONS & TYPES

Tables 3 and 4 list the relays operating time calculated by using (2) in case of different fault locations for both grid-connected and islanded modes of operation based on *ROCOV*. The results in Table 3 and 4 show that the required *CTI* is maintained between all primary and backup relays for all tested fault locations (F1 to F13 in Fig. 3) for both grid-connected mode (53 pairs of primary and backup relays) and islanded mode (51 pairs). As shown in the tables, the minimum and maximum recorded *CTI* for grid-connected mode was 0.2033 and 0.7645 s respectively, while the recorded *CTI* in islanding mode was in the range between 0.2 and 0.4582 s.

TABLE 3. Operating time of *ROCOV* relays in grid-connected mode.

Fault location	Primary relay			Backup relays			*CTI* sec
	Relay No.	|*ROCOV*| (Volt/s)×10^6	*t(op)* sec	Relay No.	|*ROCOV*| (Volt/s)×10^6	*t(op)* sec	
F1	R1	3.8	1.7893	R4	2.85	2.2850	0.4957
				R32	3.8	2.0166	0.2273
				R33	3.8	2.0196	0.2303
	R2	6	1.7922	R6	3.2	2.2679	0.4757
				R27	6	2.0170	0.2248
F2	R3	4	1.7668	R2	3.4	2.2070	0.4402
				R32	4	1.9783	0.2115
				R33	4	1.9812	0.2144
	R4	5.33	1.8233	R8	3.6	2.3066	0.4833
				R12	3.35	2.4059	0.5826
				R28	5.33	2.1446	0.3213
F3	R5	5	1.9359	R1	2.2	2.2534	0.3175
				R27	5	2.1471	0.2112
	R6	4.8	1.9637	R7	2.7	2.4257	0.462
				R10	3.5	2.5021	0.5384
F4	R7	4.5	2.0034	R12	3.4	2.3926	0.3892
				R28	4.5	2.2705	0.2671
				R3	2.18	2.2781	0.2747
	R8	5.2	2.0335	R5	2.88	2.4009	0.3674
				R10	4	2.3842	0.3507
F5	R9	6.34	1.9245	R5	2.84	2.4155	0.491
				R7	3	2.3250	0.4005
	R10	7.5	1.9486	R20	5.1	2.2522	0.3036
				R29	7.5	2.1544	0.2058
F6	R11	4	2.1501	R3	1.9	2.4367	0.2866
				R28	4	2.3658	0.2157
				R8	2.94	2.4993	0.3492
	R12	6	1.9718	R14	4.4	2.3213	0.3495
				R24	4	2.6987	0.7269
F7	R13	6.5	2.1833	R11	2.4	2.6252	0.4419
				R24	4.4	2.6037	0.4204
	R14	7.6	1.9536	R30	7.6	2.3243	0.3707
				R16	5.2	2.2351	0.2815
F8	R15	6.9	2.1891	R13	4	2.5597	0.3706
				R30	6.9	2.3924	0.2033
	R16	7.35	2.0056	R18	4.2	2.3672	0.3616
F9	R17	7.6	2.0777	R15	4.6	2.4944	0.4167
	R18	6.58	2.0506	R19	3.6	2.4472	0.3966
				R22	4.61	2.4126	0.362
F10	R19	6.56	2.0041	R9	3.5	2.3485	0.3444
				R29	6.55	2.2429	0.2388
	R20	7.5	2.0024	R17	5.2	2.3385	0.3361
				R22	5	2.3433	0.3409
F11	R21	4.2	2.2848	R17	3.35	2.7328	0.448
				R19	2.67	2.7469	0.4621
	R22	6.8	2.1124	R25	3.48	2.6075	0.4951
F12	R23	4.25	2.1176	R11	1.95	2.8821	0.7645
				R14	3.37	2.5578	0.4402
	R24	6.55	2.2687	R31	6.55	2.4750	0.2063
				R26	4	2.6410	0.3723
F13	R25	5.2	2.2431	R31	5.2	2.6744	0.4313
				R23	2.4	2.6364	0.3933
	R26	5.8	2.3109	R21	2.5	2.7751	0.4642

The results ensure the capability to get a complete coordinated protection system using *ROCOV* relays. As an example, a three-phase fault is applied at F3 in grid- connected mode, the calculated *ROCOV* value using (1) at the primary relay R5 is 5×10^6 Volt/s and at the backup relay R1 is 2.2×10^6 Volt/s. Based on the relays settings (*TDS* and pickup value) mentioned in Table 2, the relays operating time using

TABLE 4. Operating time of *ROCOV* relays in islanding mode.

	Primary relay			Backup relays			*CTI* sec
	Relay No.	$\|ROCOV\|$ (Volt/s)×10⁶	*t(op)* sec	Relay No.	$\|ROCOV\|$ (Volt/s)×10⁶	*t(op)* sec	
F1	R1	6	1.5507	R4	3.42	1.7507	0.2
				R32	6	1.8514	0.3007
	R2	6.1	1.5952	R6	3.55	1.7952	0.2
				R27	6	1.8404	0.2452
F2	R3	6.5	1.5981	R2	4.33	1.7981	0.2
				R32	6.5	1.7981	0.2
	R4	5.37	1.4949	R8	3.9	1.8395	0.3446
				R12	3.4	1.9396	0.4447
				R28	5.37	1.8836	0.3887
F3	R5	6.5	1.5928	R1	4.2	1.7928	0.2
				R27	6.5	1.7928	0.2
	R6	5.45	1.5514	R7	3.7	1.9106	0.3592
				R10	4	1.8704	0.319
F4	R7	5.75	1.6462	R12	3.9	1.8461	0.2
				R28	5.75	1.8461	0.2
				R3	4.29	1.8461	0.2
	R8	6	1.5961	R5	4.35	1.8300	0.2339
				R10	4.5	1.7961	0.2
F5	R9	7.29	1.6073	R5	4.5	1.8073	0.2
				R7	4.33	1.8073	0.2
	R10	7.45	1.5339	R20	5.5	1.7339	0.2
				R29	7.45	1.7928	0.2589
F6	R11	5.6	1.6296	R3	3.78	1.9372	0.3076
				R28	5.5	1.8692	0.2396
				R8	4	1.8296	0.2
	R12	6.1	1.5941	R14	4.75	1.7941	0.2
				R24	4.31	1.9781	0.384
F7	R13	7.2	1.6756	R11	3.7	1.8756	0.2
				R24	5	1.8756	0.2
	R14	7.56	1.5541	R30	7.56	1.8481	0.294
				R16	5.8	1.7541	0.2
F8	R15	7.2	1.6749	R13	5	1.8749	0.2
				R30	7.2	1.8749	0.2
	R16	7.6	1.6159	R18	5.1	1.8159	0.2
F9	R17	7.65	1.6368	R15	5.35	1.8368	0.2
	R18	7	1.6485	R19	4.67	1.8484	0.2
				R22	5.3	1.8485	0.2
F10	R19	7.2	1.6143	R9	4.93	1.8143	0.2
				R29	7.2	1.8144	0.2001
	R20	7.5	1.5801	R17	5.8	1.7801	0.2
				R22	5.5	1.8252	0.2451
F11	R21	5	1.6468	R17	4.15	1.9895	0.3427
				R19	3.56	2.0319	0.3851
	R22	7	1.6867	R25	4.1	1.8867	0.2
F12	R23	5.28	1.5715	R11	3	2.0297	0.4582
				R14	4.2	1.8716	0.3001
	R24	6.75	1.6970	R31	6.75	1.8970	0.2
				R26	4.75	1.8970	0.2
F13	R25	5.8	1.6694	R31	5.8	1.9928	0.3234
				R23	3.2	1.8694	0.2
	R26	6.47	1.7083	R21	3.26	1.9083	0.2

(2) are calculated as 1.9359 s and 2.2534 s for primary and backup relay respectively, while the *CTI* is above 0.2 s.

The performance of the proposed coordination system is also examined for different fault types. For brevity, Table 5 shows a sample of the primary/backup relay operating times in case of different symmetrical/unsymmetrical fault types (2L-G, 3L, 1L-G, L-L) and locations in both grid connected and islanded modes of operation while using the proposed relay. The results ensure the capability to get a complete coordinated protection system using *ROCOV* relays (all the *CTI* values are above 0.2 s) in case of different fault types and locations.

TABLE 5. Sample of the operating time of *ROCOV* relays for different fault types and locations in grid-connected and islanded modes of operation.

Fault type / mode of operation	Fault location	Primary relay			Backup relays			*CTI* sec
		Relay No.	$\|ROCOV\|$ (Volt/s)× 10⁶	*t(op)* sec	Relay No.	$\|ROCOV\|$ (Volt/s)× 10⁶	*t(op)* sec	
2L-G Islanded Mode	F1	R1	4.2	1.7928	R4	2.26	2.0689	0.2761
					R32	4.2	2.0989	0.3061
		R2	4.34	1.7966	R6	2.34	2.1157	0.3192
					R27	4.34	2.0606	0.2640
	F2	R3	4.8	1.7720	R2	3	2.0792	0.3072
					R32	4.8	1.9991	0.2270
		R4	3.72	1.6974	R8	2.6	2.1446	0.4472
					R12	2.24	2.2906	0.5932
					R28	3.72	2.1340	0.4366
3L Islanded Mode	F3	R5	5.82	1.6519	R1	3.65	1.9096	0.2577
					R27	5.82	1.8591	0.2072
		R6	4.865	1.6095	R7	3.23	2.0095	0.4000
					R10	3.465	1.9694	0.3599
	F4	R7	5.1	1.7108	R12	3.4	1.9396	0.2289
					R28	5.1	1.9153	0.2045
					R3	3.75	1.9433	0.2325
		R8	5.37	1.6526	R5	3.8	1.9260	0.2734
					R10	3.95	1.8787	0.2261
1L-G Grid-connected mode	F6	R11	4.05	2.1406	R3	1.9	2.4367	0.296
					R28	4.05	2.3554	0.2148
					R8	2.92	2.5061	0.3654
		R12	6	1.9718	R14	4.5	2.3034	0.3316
					R24	4	2.6987	0.7269
	F7	R13	6.6	2.1732	R11	2.4	2.6252	0.452
					R24	4.4	2.6037	0.4305
		R14	7.52	1.9552	R30	7.52	2.3316	0.3764
					R16	5.16	2.2409	0.2857
2L Grid-connected mode	F11	R21	1.09	4.197	R17	1.03	4.9236	0.7266
					R19	0.97	4.6524	0.4554
		R22	1.17	4.7552	R25	1.04	5.0208	0.2657
	F12	R23	1.1	3.9349	R11	0.855	4.6843	0.7494
					R14	1.03	4.6188	0.6839
		R24	1.165	5.0536	R31	1.165	5.4928	0.4393
					R26	1.07	5.2648	0.2112

TABLE 6. Different scenarios for testing the proposed coordination scheme.

Examined Scenarios	
Scenario 1	Disconnecting 3 DGs at buses 28, 30 & 32 in grid-connected mode.
Scenario 2	Disconnecting all DGs in grid-connected mode.
Scenario 3	Disconnecting line 11 in grid-connected mode.
Scenario 4	Increasing short circuit level in grid-connected mode by adding 2 DGs at buses 4 &11.
Scenario 5	Increasing short circuit level in islanded mode by adding 2 DGs at buses 4 & 11.

B. PERFORMANCE OF PROPOSED COORDINATION SCHEME WITH DIFFERENT TOPOLOGIES

The system operating conditions are likely to undergo frequent changes because of dynamically changing loads and generations. Further, topological changes can be caused by scheduled outage (for maintenance purpose) of any line or distributed generators from the live network. All these changes in the system severely affect any proper coordination using traditional DOCRs and clearly decrease the overall system reliability [35].

The performance of the proposed coordination scheme is examined with different scenarios in both grid-connected and islanded modes under different short circuit levels. The changes in network topology are simulated as described in Table 6.

For each scenario, three phase faults are applied on different feeders in the studied network (F1 to F13), and therefore a sum of sixty five fault cases are extensively investigated. The demonstrated results in Table 7 compare the calculated *CTI* using traditional DOCRs with the calculated *CTI* using proposed *ROCOV* relays for all tested fault locations in the aforementioned scenarios. According to the topological changes in tested scenarios, some relays are cancelled from the network in some fault cases and accordingly the corresponding *CTI* are excluded in Table 7, as indicated by the sign "–", *e.g.* *CTI* between R32 and R3 in Scenarios 1 and 2 for fault F2.

The results show that the traditional DOCRs failed to keep the protection system coordinated in many fault cases (*CTI* is less than 0.2 s) as illustrated in all shaded cells in Table 7. In some cases with traditional DOCRs, the operating time of backup relay was less than the operating time of primary relay and hence the backup DOCR acts before the primary DOCR. The *CTI* in such cases got a negative value and was indicated in brackets in shaded cells, *e.g.* between R8 & R4 for F2 in Scenario 2.

As an example, where the line 11 is disconnected from the network in Scenario 3, the *CTI* for all 13 fault locations based on *ROCOV* was above 0.2 s (46 coordinated pairs) while the *CTI* with some DOCRs was less than 0.2 s for 15 DOCRs pairs, *e.g.* between R15 & R17, R19 & R18 for F9 or R14 & R23, R31 & R24 for F12 …etc.

In Scenario 4, the total short circuit level is increased due to adding two DGs to the network in grid-connected mode, miscoordination cases are expected based on traditional DOCRs as between R4 & R1 for F1 (backup relay R4 acts before the primary relay R1) and between R6 & R2 for F2 (the primary relay R2 acts before the backup relay R6, but the *CTI* is less than 0.2 s), while the *CTI* for all fault locations based on *ROCOV* was above 0.2 s.

In Scenario 5, for islanded mode, two DGs are added to the network. Many miscoordination cases are noticed with DOCRs (conventional scheme) or with FCLs while the *CTI* was above 0.2 s for all fault locations based on *ROCOV* relays. Samples for this miscoordination cases are:

- The miscoordination between R24 & R26 for F12 when using traditional DOCRs. The backup relay R26 operates before the primary relay R24.
- The miscoordination between R14 & R16 for F7. The primary relay R14 acts before the backup relay R16 when using traditional DOCRs, and the *CTI* is less than 0.2 s.

For better illustration, the number of miscoordinated pairs for DOCRs and *ROCOV* relays in each tested scenario is summarized in the last row of Table 7. As clearly shown, the proposed scheme based on *ROCOV* relays is kept successfully coordinated for all the primary/backup relays, considering different operating scenarios. As shown, all *CTI* are equal or greater than 0.2 s for different fault locations, different short circuit levels and different network topologies. Thus, the achieved results have proved the selectivity feature of the proposed scheme.

It is noteworthy that the changes in the network topology or mode of operation affect the measured voltage at different buses slightly, unlike the effects on the fault current flowing in the network feeders. This adds a positive feature to the proposed scheme since it will not be affected by the variation in the network topology or changes in the mode of operation.

V. COMPARISON BETWEEN THE PROPOSED SCHEME AND OTHER TECHNIQUES

To further test and evaluate the performance of the proposed coordination scheme using *ROCOV* relays versus other existing techniques, a comprehensive comparison is carried out against the following schemes:

- The conventional protection scheme using traditional DOCRs with two settings for grid-connected and islanded modes [6],
- The conventional protection scheme using traditional DOCRs integrated with FCLs [5].

Such comparison will cover the effect of adding extra synchronous-based DGs, the effect of using inverter-based DGs and the effect of applying high fault resistance as will be presented in the following sections.

A. EFFECT OF ADDING EXTRA SYNCHRONOUS-BASED DGs

In this section, a comparison between the conventional protection schemes and the proposed scheme in terms of *CTI* is presented in Fig. 4 for adding two additional DGs at buses 4 & 11 in grid-connected mode. Such added DGs have the same rating of 2.4 MVA similar to the other existing six synchronous DG units.

The figure demonstrates the coordination time intervals for 53 primary-backup pairs for all 13 tested fault locations as indicated in Fig. 3. As illustrated, miscoordination cases are recorded between primary and backup relays for both traditional tested DOCRs schemes without/with FCL. The figure shows that some *CTI*s are less than 0.2 s with these conventional systems such as at order 27, 48 and 50 of primary-backup pairs. Some other *CTI*s show negative values with the conventional systems which means the operating time of the backup relay is less than the operating time of primary relay such as at order 1, 6 and 16 of primary-backup pairs for conventional scheme without FCL and 3, 8 and 12 of primary-backup pairs for conventional using FCL. On the other hand, the proposed coordination scheme shows proper coordination

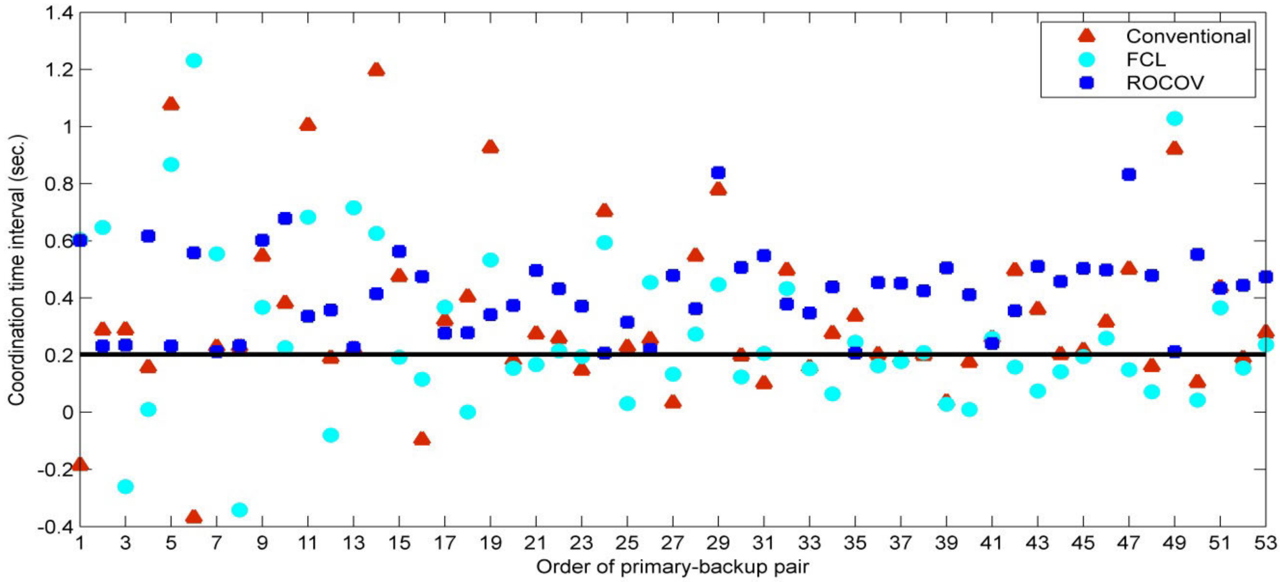

FIGURE 4. The *CTIs* in the three systems in case of adding extra synchronous-based DGs.

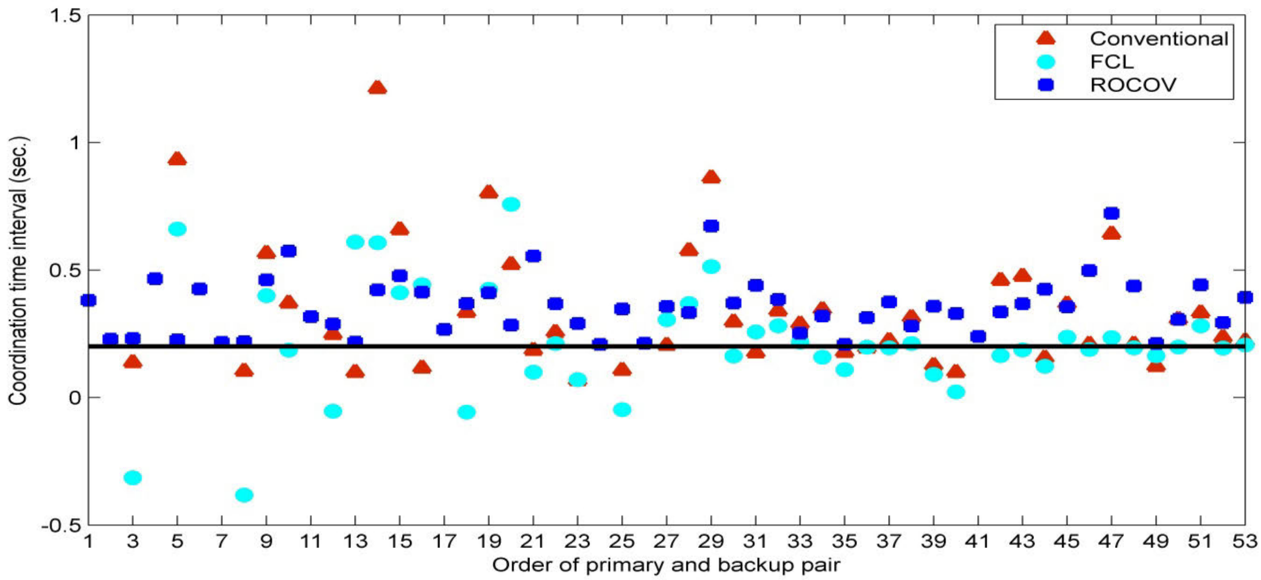

FIGURE 5. The *CTIs* n the three systems in case of using inverter based DG.

with the *CTI*s equal or greater than 0.2 s for all tested fault locations.

B. EFFECT OF USING INVERTER-BASED DGS

To further evaluation of the proposed scheme, the three synchronous-based DGs (each is 2.4 MVA) at buses 1, 3 & 5 in grid-connected are replaced by three inverter-based DGs, each is 0.1 MW. The inverter based DGs are selected with very low power rating of 0.1 MW DG size to simulate a very low fault current contribution case. The data for these added DGs is in [36]. Three phase faults are applied at all system feeders (F1 – F13) as indicated in Fig. 3. The resulted *CTIs* calculated by the proposed *ROCOV* relays are compared against traditional DOCRs in Fig. 5.

The miscoordination cases are recorded between primary and backup relays for both conventional DOCRs schemes without/with FCL. The results show that 39.6% and 62.2% of the total number of pairs are miscoordinated for conventional schemes without/with FCL respectively. Again, the proposed coordination scheme is kept successfully coordinated for all the primary/backup relays. It is concluded that, the proposed scheme has high performance with any type of DGs: inverter-based DGs or synchronous-based DGs.

TABLE 7. Primary-backup time intervals under different scenarios with different fault locations based on DOCRs and *ROCOV* relays.

Fault location	Primary relay No.	Backup relay No.	Scenario 1		Scenario 2		Scenario 3		Scenario 4		Scenario 5	
			CTI in sec		*CTI* in sec		*CTI* in sec		*CTI* in sec		*CTI* in sec	
			For DOCR	For *ROCOV*	For DOCR	For *ROCOV*	For DOCR	For *ROCOV*	For DOCR	For *ROCOV*	For DOCR	For *ROCOV*
F1	R1	R4	Non	0.3607	1.3717	0.2	0.1747	0.5004	(-0.1855)	0.6017	0.1208	0.2599
		R32	–	–	–	–	0.2593	0.2275	0.288	0.2319	0.2619	0.3028
		R33	0.1402	0.2175	–	–	0.2596	0.2305	0.2889	0.235	–	–
	R2	R6	0.2947	0.3444	0.2588	0.2	0.2047	0.4713	0.1569	0.6165	0.0773	0.3118
		R27	0.9681	0.2191	–	–	1.0239	0.2282	1.0763	0.2316	0.435	0.2438
F2	R3	R2	1.1244	0.4046	(-0.2044)	0.2	0.2364	0.4484	(-0.3694)	0.558	0.1612	0.2831
		R32	–	–	–	–	0.2032	0.2106	0.2282	0.2115	0.2945	0.2082
		R33	0.1048	0.2067	(-0.0064)	0.2	0.1990	0.2135	0.2289	0.2332	–	–
	R4	R8	0.481	0.4559	(-0.2552)	0.2999	0.6244	0.4822	0.547	0.6022	0.0818	0.4352
		R12	0.5479	0.48	15.6174	0.2885	0.4407	0.5952	0.3821	0.6785	0.1372	0.5207
		R28	–	–	–	–	0.9286	0.3228	1.0046	0.3363	0.4495	0.4003
F3	R5	R1	0.2597	0.2038	0.0892	0.2	0.1980	0.3092	0.1896	0.3576	0.1798	0.239
		R27	0.1057	0.2083	–	–	0.2028	0.2121	0.2215	0.2266	0.2476	0.209
	R6	R7	1.3191	0.319	1.2862	0.292	1.1177	0.4850	1.1961	0.4147	0.7871	0.3629
		R10	0.5518	0.4758	1.8546	0.3469	0.5301	0.5206	0.4755	0.563	0.2488	0.3617
F4	R7	R12	0.7583	0.326	(-6.0085)	0.2	0.0932	0.4206	(-0.0958)	0.4747	0.0951	0.27
		R28	–	–	–	–	0.2920	0.2723	0.3209	0.2769	0.2817	≈0.2
		R3	0.3105	0.2366	0.2422	0.2172	0.3976	0.2525	0.4045	0.2788	0.4261	0.2116
	R8	R5	0.8746	0.3101	0.9293	0.2	0.8062	0.3689	0.9263	0.3416	1.1479	0.2208
		R10	0.3381	0.3029	11.3662	0.2	0.2374	0.3388	0.1803	0.3738	0.3644	0.2239
F5	R9	R5	0.1793	0.3955	0.276	0.2847	0.2068	0.4928	0.2746	0.4963	0.3063	0.2081
		R7	0.2958	0.2508	0.3072	0.2	0.1863	0.4522	0.2588	0.4325	0.2827	0.2314
	R10	R20	0.3523	0.2173	0.1537	0.2	0.2519	0.2539	0.1477	0.3711	0.0883	0.2502
		R29	0.5526	0.2043	–	–	0.6056	0.2041	0.7033	0.2071	0.4589	0.263
F6	R11	R3	0.1349	0.2351	0.0604	0.2	0.2039	0.2997	0.2283	0.315	0.2153	0.3378
		R28	–	–	–	–	0.2087	0.2157	0.2549	0.2197	0.3015	0.235
		R8	0.109	0.3495	1.0381	0.2	0.1686	0.3766	0.0332	0.4788	0.0397	0.2885
	R12	R14	0.7212	0.247	0.5512	0.2	0.5009	0.3588	0.5467	0.3622	0.3098	0.2671
		R24	0.7711	0.6669	1.4382	0.4617	0.9908	0.6319	0.7786	0.8386	0.4292	0.4809
F7	R13	R11	0.2826	0.2923	0.2737	0.2	0.1741	0.4599	0.1974	0.5065	0.1533	0.2671
		R24	0.1697	0.4097	1.3283	0.2	0.3133	0.3609	0.1008	0.5484	0.1307	0.2987
	R14	R30	–	–	–	–	0.4643	0.3767	0.4971	0.3782	0.2653	0.2984
		R16	0.0745	0.2499	0.1159	0.2001	0.1844	0.3077	0.1567	0.3476	0.0533	0.2513
F8	R15	R13	0.2052	0.3136	0.2201	0.2	0.2875	0.4061	0.2757	0.4384	0.2013	0.2622
		R30	–	–	–	–	0.3145	0.2044	0.3366	0.2072	0.2761	0.2158
	R16	R18	0.1961	0.3126	0.1789	0.2	0.1982	0.3328	0.202	0.4539	0.236	0.2772
F9	R17	R15	0.2703	0.2786	0.3639	0.2	0.1821	0.4940	0.1877	0.4512	0.1597	0.2334
	R18	R19	0.239	0.3256	0.3841	0.2001	0.1195	0.4192	0.1993	0.4247	0.1667	0.258
		R22	0.276	0.3127	(-0.4188)	0.2	-	-	0.0364	0.5051	0.0271	0.3425
F10	R19	R9	0.2505	0.2557	0.1122	0.2	0.1889	0.3731	0.1748	0.4113	0.1661	0.2671
		R29	0.1167	0.2352	–	–	0.2144	0.2395	0.2594	0.2406	0.3219	0.2018
	R20	R17	0.4937	0.2458	0.3975	0.2001	0.2978	0.3892	0.4967	0.3556	0.4068	0.2204
		R22	0.4342	0.2724	0.6951	0.2061	-	-	0.3604	0.5111	0.1929	0.3894
F11	R21	R17	0.364	0.3519	0.4087	0.3272	-	-	0.2025	0.4578	0.2685	0.3522
		R19	0.2493	0.4039	0.4162	0.2923	-	-	0.2165	0.5039	0.3008	0.4384
	R22	R25	0.2196	0.3759	0.3006	0.2001	-	-	0.3162	0.4978	0.3399	0.2148
F12	R23	R11	0.5796	0.6206	0.6585	0.5314	0.5268	0.8510	0.5016	0.8318	0.3419	0.537
		R14	0.4209	0.3451	0.8175	0.3025	0.0955	0.5634	0.1606	0.4788	0.1888	0.3402
	R24	R31	0.145	0.2049	–	–	(-0.1942)	0.2011	0.9212	0.2122	0.297	0.2033
		R26	0.2976	0.2748	0.0261	0.2	-	-	0.1045	0.5521	(-0.045)	0.3514
F13	R25	R31	0.3384	0.4155	–	–	0.5362	0.4736	0.4365	0.4341	0.4708	0.325
		R23	0.2481	0.5091	0.1134	0.2	0.1551	0.8128	0.1883	0.4446	0.1863	0.2378
	R26	R21	0.2091	0.333	0.223	0.2001	-	-	0.2788	0.4741	0.3234	0.2081
No. of miscoordinated primary-backup pairs			11 pairs	zero	13 pairs	zero	15 pairs	zero	18 pairs	zero	20 pairs	zero

C. EFFECT OF HIGH FAULT RESISTANCE

An efficient protection scheme must be sensitive enough to detect high resistance faults, which may have current magnitudes close to normal magnitude values. The conventional overcurrent and under voltage relays may not be able to detect such faults [37]. Refer to Fig. 3, a three-phase fault is simulated at F1 with a fault resistance of 30 ohms at line 1. The conventional overcurrent and under voltage relays couldn't

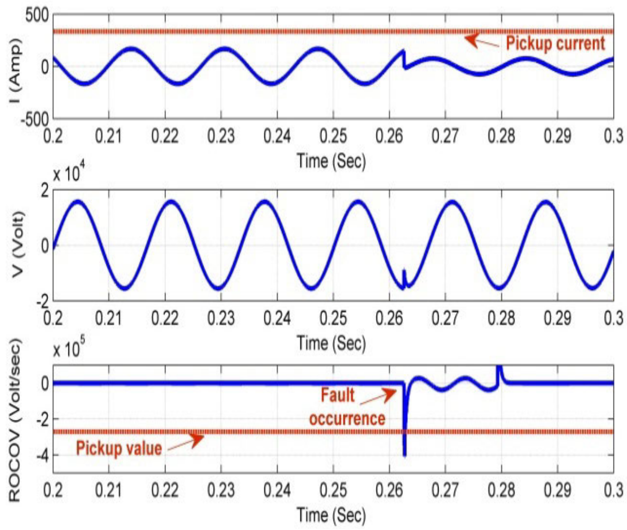

FIGURE 6. Current, voltage and *ROCOV* responses in case of a fault with 30 ohms fault resistance at line 1.

TABLE 8. Optimum four settings of *ROCOV* relays achieved by the proposed coordination scheme in grid-connected mode.

Grid-connected mode				
Relay	TDS (s)	$ROCOV_{pick-up}$ (Volt/s) $\times 10^5$	A	B
1	1.4565	4.1963	18.3269	1.9707
2	1.3095	4.7005	3.7576	0.9674
3	1.2948	3.1858	46.8144	1.9997
4	1.4982	4.4000	37.2288	1.9641
5	1.1579	4.846	15.9966	1.5238
6	0.6538	2.1916	2.3192	0.388
7	1.4977	4.4000	2.4005	0.7493
8	1.0321	2.1528	2.1466	0.4824
9	1.4994	4.2298	12.2074	1.2388
10	0.0529	2.976	0.574	0.0127
11	1.4974	4.4	9.3422	1.3729
12	0.8518	2.1812	2.8477	0.4211
13	1.4994	4.2901	22.296	1.3715
14	1.4881	2.3609	3.5476	0.5707
15	1.4844	4.3117	17.2114	1.1911
16	1.4992	4.4998	0.1032	0.0521
17	1.2781	3.2391	5.1636	0.6685
18	1.4996	4.0973	0.0441	0.0207
19	1.4999	4.3	16.2707	1.2263
20	1.4996	4.1	6.8428	0.8978
21	1.2074	3.673	1.2313	0.3257
22	0.1658	5.4186	0.1976	0.0101
23	1.4951	4.2916	5.6173	0.9267
24	1.2353	2.8058	8.0054	0.785
25	1.5	5.3987	4.8425	0.7999
26	0.7328	2.7376	0.691	0.1179
27	0.4284	2.8786	0.3284	0.0565
28	1.4735	3.7499	2.3998	0.5976
29	0.7589	3.4503	1.2984	0.1491
30	0.2313	2.2725	0.5222	0.0111
31	1.419	5.1386	3.185	0.601
32	1.368	4.3762	3.5242	0.691
33	0.2934	2.525	0.26	0.0266

detect such fault as illustrated in the first and second graphs of Fig. 6 since the measured fault current is less than the pickup current and the voltage almost does not change. On the other hand, the proposed primary *ROCOV* relay R2 was able to detect such fault. The *ROCOV* value has exceeded the pickup value as shown in the third graph of Fig. 6. The previous case ensured the effectiveness of the proposed protection scheme using *ROCOV* relay over the conventional techniques based on the current or voltage even. The results also proved the sensitivity of the proposed technique.

TABLE 9. Optimum four settings of *ROCOV* relays achieved by the proposed coordination scheme in islanded-mode.

Islanded mode				
Relay	TDS (s)	$ROCOV_{pick-up}$ (Volt/s) $\times 10^5$	A	B
1	1.3894	3.693	6.9413	1.0822
2	0.186	2.909	1.0584	0.0715
3	1.495	3.1608	1.0692	0.3917
4	0.4352	2.3945	3.0756	0.3962
5	1.3306	4.7502	7.0213	1.1203
6	0.7168	2.4723	1.1596	0.222
7	0.5844	3.2665	15.3528	0.9253
8	1.4942	2.1594	0.5104	0.2381
9	1.3655	3.5879	7.5046	1.0293
10	1.4578	2.3654	10.8815	0.979
11	0.78	2.1715	0.4469	0.1301
12	1.4996	3.9241	2.4648	0.7103
13	1.4763	4.1375	26.2074	1.6296
14	1.3087	4.3509	6.0385	0.9827
15	1.4869	4.38	22.9518	1.545
16	1.1412	4.2248	8.1011	0.9968
17	1.3108	4.3124	17.302	1.3277
18	1.4975	3.9956	6.6203	1.033
19	1.1178	2.3927	7.2351	0.8247
20	1.3924	4	14.41	1.2532
21	1.4276	2.7414	0.1056	0.0635
22	1.3748	4.4587	3.4051	0.7913
23	0.5266	2.0909	2.3846	0.3723
24	1.4449	5.2	34.6466	1.943
25	1.1904	3.933	20.1006	1.4549
26	1.3327	5.0063	37.5899	1.9566
27	0.6266	2.8342	1.1411	0.0464
28	0.6137	2.1736	0.9924	0.078
29	0.3034	2.1246	0.2039	0.0214
30	0.6543	2.2224	0.3286	0.0725
31	1.0289	2.8514	0.7571	0.2666
32	1.245	2.8748	1.1113	0.0918

VI. PROPOSING USER-DEFINED CHARACTERISTICS FOR MICROGRID PROTECTION COORDINATION USING ROCOV RELAYS

Furthermore, the *ROCOV* relay parameters that define characteristics shape (*A* and *B*) can be optimized. In this section, the proposed coordination strategy will consider the four settings for relay characteristics (TDS, pickup, *A* and *B*) as continuous variable settings that can be adjusted to achieve coordination. The coordination problem is reformulated as a nonlinear programming problem where the main objective is to minimize the overall time of operation of relays during primary and backup operation considering faults at different locations. The proposed approach is also verified by MATLAB simulation on the same modified IEEE 14 bus system embedded with DGs previously shown in Fig. 3.

In addition to considering the constraints of Equations (5)-(6) for minimum and maximum pick-up and TDS settings (previously discussed in Section II), the following constraints

TABLE 10. Relays operating time for different fault locations based on *ROCOV* relays with four optimized settings in grid-connected mode.

Fault location	Primary relay			Backup relays			CTI sec
	Relay No.	|ROCOV| (Volt/sec)×10⁶	t(op) sec	Relay No.	|ROCOV| (Volt/sec)×10⁶	t(op) sec	
F1	R1	3.8	0.3518	R4	2.85	1.4588	1.107
				R32	3.8	1.3963	1.0445
				R33	3.8	1.02	0.6682
	R2	6	0.4578	R6	3.2	0.8286	0.3708
				R27	6	0.7516	0.2937
F3	R5	5	0.5442	R1	2.2	1.0599	0.5157
				R27	5	0.8038	0.2596
	R6	4.8	0.6558	R7	2.7	1.2424	0.5866
				R10	3.5	0.9549	0.2991
F6	R11	4	0.7099	R3	1.9	1.7544	1.0444
				R28	4	1.1352	0.4253
				R8	2.94	1.02	0.31
	R12	6	0.7985	R14	4.4	1.2252	0.4267
				R24	4	1.4024	0.6039
F9	R17	7.6	0.9111	R15	4.6	1.6199	0.7088
	R18	6.58	1.118	R19	3.6	1.9459	0.8279
				R22	4.61	1.4988	0.3808
F10	R19	6.56	0.8951	R9	3.5	1.4406	0.5455
				R29	6.55	1.7884	0.8933
	R20	7.5	0.8149	R17	5.2	1.223	0.408
				R22	5	1.4434	0.6285
F13	R25	5.2	1.4182	R31	5.2	1.6566	0.2383
				R23	2.4	2.1373	0.7191
	R26	5.8	1.1686	R21	2.5	1.7136	0.545

TABLE 11. Relays operating time for different fault locations based on *ROCOV* relays with four optimized settings in islanded mode.

Fault location	Primary relay			Backup relays			CTI sec
	Relay No.	|ROCOV| (Volt/sec)×10⁶	t(op) sec	Relay No.	|ROCOV| (Volt/sec)×10⁶	t(op) sec	
F5	R9	7.29	0.4835	R5	4.5	0.8184	0.3349
				R7	4.33	0.9037	0.4201
	R10	7.45	0.5606	R20	5.5	0.7807	0.2201
				R29	7.45	0.7813	0.2207
F6	R11	5.6	0.6624	R3	3.78	0.9728	0.3104
				R28	5.5	2.1259	1.4635
				R8	4	2.9641	2.3017
	R12	6.1	0.6138	R14	4.75	0.834	0.2202
				R24	4.31	0.8358	0.222
F7	R13	7.2	0.3716	R11	3.7	0.7814	0.4097
				R24	5	0.6237	0.2521
	R14	7.56	0.5128	R30	7.56	0.738	0.2252
				R16	5.8	0.7328	0.22
F8	R15	7.2	0.4574	R13	5	0.6786	0.2211
				R30	7.2	0.7497	0.2923
	R16	7.6	0.5495	R18	5.1	0.7695	0.22
F10	R19	7.2	0.5196	R9	4.93	0.7406	0.221
				R29	7.2	0.7907	0.2711
	R20	7.5	0.5227	R17	5.8	0.7432	0.2205
				R22	5.5	0.7428	0.2201
F11	R21	5	0.7448	R17	4.15	1.1807	0.436
				R19	3.56	0.9782	0.2335
	R22	7	0.5973	R25	4.1	0.8173	0.22

are also considered for maximum and minimum values of A and B as follows:

$$A_{min} \leq A_i \leq A_{max} \tag{7}$$

$$B_{min} \leq B_i \leq B_{max} \tag{8}$$

TABLE 12. Coordination time interval under different fault locations in different scenarios based on *ROCOV* relays with four optimized settings.

			Scenario 1	Scenario 2	Scenario 3	Scenario 4	Scenario 5
Fault location	Primary relay No.	Backup relay No.	*CTI* for *ROCOV* in sec				
F1	R1	R4	0.5642	0.24	1.1261	1.573	0.2517
		R32	-	-	1.0459	1.0737	3.8566
		R33	0.7054	-	0.6674	0.6496	–
	R2	R6	0.3061	0.2402	0.3702	0.4391	0.318
		R27	0.3098	-	0.2986	0.2735	3.9708
F3	R5	R1	0.2718	0.24	0.5053	0.5994	0.2656
		R27	0.2996	-	0.2529	0.2658	4.0648
	R6	R7	0.3562	0.2877	0.6099	0.6168	0.292
		R10	0.2855	0.2418	0.2927	0.2927	0.3711
F7	R13	R11	0.3958	0.24	0.7167	0.8282	0.4314
		R24	0.4685	0.2398	0.4046	0.6079	0.47
	R14	R30	-	-	2.2002	2.2046	0.2271
		R16	0.2748	0.2408	0.3057	0.3305	0.2949
F12	R23	R11	0.5475	0.3578	1.2629	1.1491	0.3523
		R14	0.2937	0.2641	0.4198	0.3625	0.5107
	R24	R31	0.3349	-	0.3113	0.3551	0.2186
		R26	0.4016	0.3833	-	0.5238	0.6255

For the A and B constants; it has been chosen to have a minimum value of 0.01 and a maximum value of 80 and 2 respectively which represent the standardized values of the IEC 60255 standard for the very inverse time–current relay characteristics.

Accordingly, the achieved optimum four settings of relays using the proposed protection scheme for both grid-connected and islanded modes of operation are presented in Table 8 and Table 9 respectively.

For brevity, Table 10 and 11 list a sample of relays' operating time for different fault locations upon applying the optimized four settings for both grid-connected and islanded modes of operation respectively.

In the grid-connected mode of operation, the total operating time of all 33 relays was 97.1608 seconds, while in the island mode; the total operating time of all 32 relays for different faults was 77.3728 seconds. The results confirm that it is possible to obtain a shorter operating time for the protection relays through the optimized four settings while maintaining relays coordination. As an example, when a three-phase fault is applied at F3 in grid-connected mode, the calculated *ROCOV* value at the primary relay R5 is 5×10^6 Volt/s and at the backup relay R1 is 2.2×10^6 Volt/s. Based on the relays four settings (TDS, pickup, A and B) mentioned in Table 8, the relays operating time are estimated by 0.5442 s and 1.0599 s for primary and backup relay respectively, while the relays operating time based on only two optimized settings are estimated by larger operating time of 1.9359 s and 2.2534 s for primary and backup relay respectively.

Moreover, to evaluate the achieved settings, same scenarios in Table 6 (that simulate the change in short circuit level due to connection, disconnection of DGs) are applied to widely test the four settings in both grid-connected and islanded modes. Thus, sixty-five fault cases are simulated in the modified IEEE 14 system in both grid-connected and islanded modes of operation. For brevity, a sample for the performance of the proposed protection scheme based on *ROCOV* relays with four optimized settings in terms of *CTI* is examined as shown in Table 12. The results ensure proper coordination as the *CTI*s are equal or greater than 0.2 for different fault locations in all tested cases.

VII. CONCLUSION

This paper proposes a new microgrid protection scheme that is capable of operating in both grid-connected and islanded modes based only on local measurements. The protection coordination scheme depends on calculating the rate of change of fundamental voltage to detect different fault types and to estimate the proper operating time for all primary and back up relays in a meshed network.

The main contribution of the proposed coordination scheme can be summarized as follows:

- The proposed scheme can identify the faulty zone accurately and guarantee robust coordination between primary and backup relays in both grid-connected and islanded modes.
- It is robust against the change in short circuit level or change in network operating conditions.
- The proposed scheme depends only upon locally available information which means it is more reliable and dependable than those that depends upon the information at the remote ends.
- The proposed scheme does not require high sampling frequency. Actually, low sampling frequency in the range of 1-20 kHz can be applied to implement the proposed scheme.
- The full coordination scheme can be achieved by optimizing two or four settings of relay characteristic.
- Simulation results show the superiority of the proposed coordination scheme, in the presence and absence of DGs (with inverter-based DGs or with synchronous-based DGs), over conventional well-known DOCRs coordination scheme or using FCLs.
- The proposed protection scheme can maintain the coordination between primary and backup relays for different fault locations, types and different topologies.
- The results also prove the sensitivity of the proposed scheme compared to overcurrent and under voltage relays for high impedance faults.

Finally, as relays' manufactures can implement *ROCOV* relay as a new digital relay (or implement the idea as an additional feature to existing digital relays), the operators of microgrids and distribution networks can apply the proposed coordination scheme to estimate proper settings for grid-connected or islanded modes.

REFERENCES

[1] B. J. Brearley and R. R. Prabu, "A review on issues and approaches for microgrid protection," *Renew. Sustain. Energy Rev.*, vol. 67, no. 1, pp. 988–997, 2017.

[2] A. A. Memon and K. Kauhaniemi, "A critical review of AC microgrid protection issues and available solutions," *Electr. Power Syst. Res.*, vol. 129, pp. 23–31, Dec. 2015.

[3] A. Hirsch, Y. Parag, and J. Guerrero, "Microgrids: A review of technologies, key drivers, and outstanding issues," *Renew. Sustain. Energy Rev.*, vol. 90, pp. 402–411, Jul. 2018.

[4] V. Telukunta, J. Pradhan, A. Agrawal, M. Singh, and S. G. Srivani, "Protection challenges under bulk penetration of renewable energy resources in power systems: A review," *CSEE J. Power Energy Syst.*, vol. 3, no. 4, pp. 365–379, Dec. 2017.

[5] E. Dehghanpour, H. K. Karegar, R. Kheirollahi, and T. Soleymani, "Optimal coordination of directional overcurrent relays in microgrids by using cuckoo-linear optimization algorithm and fault current limiter," *IEEE Trans. Smart Grid*, vol. 9, no. 2, pp. 1365–1375, Mar. 2018.

[6] R. R. Ferreira, P. J. Colorado, A. P. Grilo, J. C. Teixeira, and R. C. Santos, "Method for identification of grid operating conditions for adaptive overcurrent protection during intentional islanding operation," *Int. J. Electr. Power Energy Syst.*, vol. 105, pp. 632–641, Feb. 2019.

[7] S. Jamali and H. Borhani-Bahabadi, "Non-communication protection method for meshed and radial distribution networks with synchronous-based DG," *Int. J. Electr. Power Energy Syst.*, vol. 93, pp. 468–478, Dec. 2017.

[8] S. Jamali and H. Borhani-Bahabadi, "Protection method for radial distribution systems with DG using local voltage measurements," *IEEE Trans. Power Del.*, vol. 34, no. 2, pp. 651–660, Apr. 2019.

[9] S. D. A. Fletcher, P. J. Norman, S. J. Galloway, and G. M. Burt, "Analysis of the effectiveness of non-unit protection methods within DC microgrids," in *Proc. IET Conf. Renew. Power Gener. (RPG)*, Sep. 2011, pp. 6–8.

[10] H. Beder, B. Mohandes, M. S. E. Moursi, E. A. Badran, and M. M. E. Saadawi, "A new communication-free dual setting protection coordination of microgrid," *IEEE Trans. Power Del.*, vol. 36, no. 4, pp. 2446–2458, Aug. 2021.

[11] S. A. Hosseini, H. A. Abyaneh, S. H. H. Sadeghi, F. Razavi, and A. Nasiri, "An overview of microgrid protection methods and the factors involved," *Renew. Sustain. Energy Rev.*, vol. 64, pp. 174–186, Oct. 2016.

[12] O. V. G. Swathika and S. Hemamalini, "Review on microgrid and its protection strategies," *Int. J. Renew. Energy Res.*, vol. 6, no. 4, pp. 1574–1587, Jan. 2016.

[13] H. Laaksonen, D. Ishchenko, and A. Oudalov, "Adaptive protection and microgrid control design for Hailuoto island," *IEEE Trans. Smart Grid*, vol. 5, no. 3, pp. 1486–1493, May 2014.

[14] A. Khademlahashy, L. Li, J. Every, and J. Zhu, "A review on protection issues in micro-grids embedded with distribution generations," in *Proc. 12th IEEE Conf. Ind. Electron. Appl. (ICIEA)*, Jun. 2017, pp. 913–918.

[15] S. Kar, S. R. Samantaray, and M. D. Zadeh, "Data-mining model based intelligent differential microgrid protection scheme," *IEEE Syst. J.*, vol. 11, no. 2, pp. 1161–1169, Jun. 2017.

[16] E. Casagrande, W. L. Woon, H. H. Zeineldin, and D. Svetinovic, "A differential sequence component protection scheme for microgrids with inverter-based distributed generators," *IEEE Trans. Smart Grid*, vol. 5, no. 1, pp. 29–37, Jan. 2014.

[17] X. Li, A. Dysko, and G. M. Burt, "Traveling wave-based protection scheme for inverter-dominated microgrid using mathematical morphology," *IEEE Trans. Smart Grid*, vol. 5, no. 5, pp. 2211–2218, Sep. 2014.

[18] H. H. Zeineldin, H. M. Sharaf, D. K. Ibrahim, and E. E.-D.-A. El-Zahab, "Optimal protection coordination for meshed distribution systems with DG using dual setting directional over-current relays," *IEEE Trans. Smart Grid*, vol. 6, no. 1, pp. 115–123, Jan. 2015.

[19] H. M. Sharaf, H. H. Zeineldin, and E. El-Saadany, "Protection coordination for microgrids with grid-connected and islanded capabilities using communication assisted dual setting directional overcurrent relays," *IEEE Trans. Smart Grid*, vol. 9, no. 1, pp. 143–151, Jan. 2018.

[20] T. S. Ustun and R. H. Khan, "Multiterminal hybrid protection of microgrids over wireless communications network," *IEEE Trans. Smart Grid*, vol. 6, no. 5, pp. 2493–2500, Sep. 2015.

[21] V. C. Nikolaidis, E. Papanikolaou, and A. S. Safigianni, "A communication-assisted overcurrent protection scheme for radial distribution systems with distributed generation," *IEEE Trans. Smart Grid*, vol. 7, no. 1, pp. 114–123, Jan. 2016.

[22] A. Rostami, H. Abdi, M. Moradi, J. Olamaei, and E. Naderi, "Islanding Detection based on ROCOV and ROCORP parameters in the presence of synchronous DG applying the capacitor connection strategy," *Electr. Power Compon. Syst.*, vol. 45, no. 3, pp. 230–315, 2017, doi: 10.1080/15325008.2016.1250842.

[23] A. Rostami, A. Jalilian, M. T. Hagh, K. M. Muttaqi, and J. Olamaei, "Islanding detection of distributed generation based on rate of change of exciter voltage with circuit breaker switching strategy," *IEEE Trans. Ind. Appl.*, vol. 55, no. 1, pp. 954–963, Jan. 2019, doi: 10.1109/TIA.2018.2868547.

[24] S. K. Salman, "New loss of mains detection algorithm for embedded generation using rate of change of voltage and changes in power factors," in *Proc. 7th Int. Conf. Develop. Power Syst. Protection (DPSP)*, Apr. 2001, pp. 82–85.

[25] M. S. Parniani, M. Sanaye-Pasand, and P. Jafarian, "A blocking scheme for enhancement of distance relay security under stressed system conditions," *Int. J. Electr. Power Energy Syst.*, vol. 94, pp. 104–115, Jan. 2018.

[26] M. Jonsson and J. Daalder, "An adaptive scheme to prevent undesirable distance protection operation during voltage instability," *IEEE Trans. Power Del.*, vol. 18, no. 4, pp. 1174–1180, Oct. 2003, doi: 10.1109/MPER.2002.4311847.

[27] M. Sharifzadeh, H. Lesani, and M. Sanaye-Pasand, "A new algorithm to stabilize distance relay operation during voltage-degraded conditions," *IEEE Trans. Power Del.*, vol. 29, no. 4, pp. 1639–1647, Aug. 2014.

[28] M. A. Dawoud, D. K. Ibrahim, M. I. Gilany, and A. El'gharably, "Proposed application for rate of change of phasor voltage in fault detection and coordination studies in MV distribution networks," *Iranian J. Sci. Technol., Trans. Electr. Eng.*, vol. 45, no. 3, pp. 815–831, Sep. 2021.

[29] Y. Wang and V. Dinavahi, "Real-time digital multi-function protection system on reconfigurable hardware," *IET Gener., Transmiss. Distrib.*, vol. 10, no. 10, pp. 2295–2305, Jul. 2016.

[30] M. A. Dawoud, D. K. Ibrahim, M. I. Gilany, and A. El'gharably, "A proposed passive islanding detection approach for improving protection systems," *Int. J. Renew. Energy Res.*, vol. 10, no. 4, pp. 1940–1950, Dec. 2020.

[31] L. Huchel and H. H. Zeineldin, "Planning the coordination of directional overcurrent relays for distribution systems considering DG," *IEEE Trans. Smart Grid*, vol. 7, no. 3, pp. 1642–1649, May 2016.

[32] Z. Abdmouleh, A. Gastli, L. Ben-Brahim, M. Haouari, and N. A. Al-Emadi, "Review of optimization techniques applied for the integration of distributed generation from renewable energy sources," *Renew. Energy*, vol. 113, pp. 266–280, Dec. 2017.

[33] M. N. Alam, "Adaptive protection coordination scheme using numerical directional overcurrent relays," *IEEE Trans. Ind. Informat.*, vol. 15, no. 1, pp. 64–73, Jan. 2019.

[34] A. Yazdaninejadi, D. Nazarpour, and S. Golshannavaz, "Dual-setting directional over-current relays: An optimal coordination in multiple source meshed distribution networks," *Int. J. Electr. Power Energy Syst.*, vol. 86, pp. 163–176, Mar. 2017.

[35] A. Sharma and B. K. Panigrahi, "Phase fault protection scheme for reliable operation of microgrids," *IEEE Trans. Ind. Appl.*, vol. 54, no. 3, pp. 2646–2655, May/Jun. 2018.

[36] A. Muhtar and I. W. Mustika, "The comparison of ANN-BP and ANN-PSO as learning algorithm to track MPP in PVSystem," in *Proc. 7th Int. Annu. Eng. Seminar (InAES)*, Aug. 2017, pp. 1–6.

[37] S. H. Mortazavi, Z. Moravej, and S. M. Shahrtash, "A hybrid method for arcing faults detection in large distribution networks," *Int. J. Elect. Power Energy Syst.*, vol. 94, pp. 141–150, Jan. 2018.

MOHAMED AHMED DAWOUD received the B.S. degree in electrical power engineering from the Higher Institute of Engineering, El-Shorouk City, in 2014, and the M.Sc. degree in electrical power engineering from Cairo University, Egypt, in 2017. He worked as a Demonstrator with the Electrical Power and Machines Department, Higher Institute of Engineering, El-Shorouk City, until 2019. His research interests include power system protection, microgrids, and renewable energy resources.

DOAA KHALIL IBRAHIM (Senior Member, IEEE) was born in Egypt, in December 1973. She received the M.Sc. and Ph.D. degrees in digital protection from Cairo University, Cairo, Egypt, in 2001 and 2005, respectively. From 1996 to 2005, she was a Demonstrator and a Research Assistant with Cairo University. In 2005, she became an Assistant Professor with Cairo University. In 2011, she became an Associate Professor with Cairo University. In December 2016, she became a Professor with Cairo University. From 2005 to 2008, she contributed to a World Bank Project in Higher Education Development, Egypt. From January 2010 to June 2013, she contributed as an Expert in the Program of Continuous Improvement and Qualifying for Accreditation in Higher Education in Egypt. From July 2013 to November 2014, she contributed as an Expert for the technical office of the Project Management Unit (PMU), Ministry of Higher Education, Egypt. Her research interests include digital protection of power systems, and utilization and generation of electric power, distributed generation, and renewable energy sources.

MAHMOUD IBRAHIM GILANY received the B.S. and M.S. degrees in electrical power engineering from Cairo University, Egypt, in 1987 and 1989, respectively, and the Ph.D. degree in electrical power engineering from the University of Calgary, Alberta, Canada, in 1993. Since 1993, he has been a Faculty Member of the Faculty of Engineering, Cairo University. His research interests include power system protection, power quality, and smart networks.

ABOUL'FOTOUH EL'GHARABLY received the B.Sc. and M.Sc. degrees in electric power engineering from Helwan University, Egypt, in 1980 and 1984, respectively, and the Ph.D. degree in electric power engineering from Wroclaw University, Poland, in 1992. He worked as a Professor with the Electrical Power and Machines Department, Helwan University, until 2003. He is currently the Head of the Electrical Power and Machines Department, Higher Institute of Engineering, El-Shorouk City. His research interests include smart grids, power system stability, power system reliability, and renewable energy resources.